Authors would like to thank all reviewers for their time and their useful comments which enhanced the quality of the manuscript. Above answers to all the specifics comments can be found.

Referee1

Page 1, L23: The full name of AERONET in abstract should be provided when the word first appeared. What's more, Page 2, L18, the same change should be addressed in IWV.

Abbreviations are now explained in the text.

Page 3, L7-L9, some references should be provided.

References added

Page 4, L13, It is better to describe structure of this paper in the end of introduction.

A sentence has been added to describe the structure.

Page 4, L19, It would be better if you could provide an in-situ figure about PSR, which would give the reader more information

A photo of the instrument at Lindenberg, Germany has been added.

Page 4, L28, an > and

Corrected

Page 5, L1-L6, some references should be provided.

Reference added and a more detailed publication is being prepared by the authors and will be submitted in 2018.

Page 5, L8, sensors > sensor

Corrected

Page 5, L11-L12, Is there any reference to the calibration of the instrument? If so, please provide.

The calibration details are mentioned in the lines 14-17 page 5. Co-authors of this study are preparing a manuscript concerning the PSR instrument including all details of calibration procedures, characterization and measurements that is scheduled to be submitted during 2018.

Page 5, L16, what is the resolution of this instrument? How long is the interval between two consecutive observations?

A sentence has been added to clarify the measuring routine of PSR. PSR can measure multiple spectras per minute (a usual Direct sun measurement is set around 500ms). The routine used during the measuring period, saved an averaged spectrum per minute, using 5 Direct sun measurements and eliminating 5 averaged dark current recordings.

Page 5, L32, eight bandpass should be nine bandpass

This sentence has been restated

Page 5, L29, The two words (calculation in) are linked together

Corrected

Page 6, L3, the author mentioned that the photometer changed two times during the two years of observations, and whether the different numbering instruments would have a certain effect on the real water vapor retrievals?

Calibration procedures of AERONET protocol ensure the quality of the retrievals and the stability among instruments. During our study, we have separate plots for the period of each different CIMEL used, against the other instruments and statistics of the differences were the same. So, for this particular study we are confident that there are no errors related to that change, although some future study could investigate the behaviour of instruments in various AERONET stations to quantify the stability and the uncertainty introduced by the current protocol to IWV retrievals.

Page 7, L27, What version of MODTRAN used in the paper? The version number should be marked throughout the paper.

“MODTRAN 5.2.1” Is now used everywhere in the text

Page 8, L19, Section 3.2

Corrected

Page 9, L12, The references should been provided about Beer-lambert law.

Reference added

Page 9, L14, Get rid of this extra arrow

Corrected

Page 10, L10, Why author selected the mid-latitude built?

Preset atmospheres in MODTRAN 5.2.1 include Tropical, Midlatitude, Sub-Arctic and 1976 Standard US. Since no info about the vertical structure of the atmosphere

could be used to have an estimation for the selection, we used the Midaltitude built among those. Ingold et al. (2000) demonstrate a ~0.05% change of the coefficients used according to the selection of the preset atmosphere, but still they found a more important variation due to changes in altitude. A future enhancement of the method could include some input info about atmospherical structure and a following selection of the set of coefficients.

Page 11, L15-L18, These sentences repeat with the previous text, please check

The first sentence has been deleted

Page 13, L16,L19, Figure 4 > Figure 5

Figure numbers have been updated an corrected.

Page 14, L12, Figure 6, MW > MWP

corrected

Page 15,L19, comparing results > comparison results

Corrected

Page 16, L3,L6, Equation (3) should be Equation (9)

Equation (3) is repeated here, to help the reader follow the uncertainty analysis. If it is against the journal policy to repeat the same equation, it could be deleted.

Page 18, L17, 0.02cm > 0.01 cm? Please check

Corrected

Page 18, L18, 0.16 > 0.17? Please check

Corrected

Page 18, L19, 3cm > 3

Corrected

Page 18, L32, some relevant statistical variables should been defined in table

Table 1 shows the effect described in this sentence by the larger values of the standard deviation and the 10-90 percentiles for the radiosonde-PSR compare to the other instrument vs PSR comparisons.

Page 19, L6, Figure 8 > Figure 9

Figure numbers have been updated and corrected.

Page 19, L11-L12, Some explanations or references are needed.

The sentence has been restated to be clear that at higher AOD values, the uncertainty of the extrapolated value is larger thus higher deviations could be sourced to this fact.

Page 19, L17, below 2cm?

Since the quantity of IWV (GPS-PSR)/ PSR is illustrated, negative points are the ones that PSR is overestimating. The ones of overestimation higher than 0.2 are mainly found when IWV>0.2cm.

Page 20,22, Figure 9, Figure 11, numver > number.

Corrected

Page 22, L1, redundant sentence, please remove it.

The sentence has been removed

Page 23, L7, other instrumens (CIMEL, MWP, GPS, and radiosonde) have been

The sentence has been restated

Referee 2

p3, l15: the number of current stations is much higher, please update the figure (currently over 500).

The sentence has been updated.

- p4: a slightly more in depth description of new PSR would be good, including a scheme or image. –

An image of the instrument has been added and a sentence for the measuring/archiving routine. A more detailed publication for the technical characteristics of the instrument is being prepared from the authors.

p5, l29: "calculations in" –

corrected

p12, figure 3: figure could include not only the average for all the wavelengths but also the IWV for the reference wavelength 946nm. –

A reference line for retrievals at 946nm has been added and a sentence in the text to describe it.

p13, figure 4: the limits of the bands could be included for a better illustration

Since the aim of the study is PSR retrievals and PSR bands are continuous in the spectral region of 300-1020 we think that pointing that in the figure would not provide additional information. WMO recommendations are included in previous general plot. The aim of this figure is to point the potential of using a wider spectral range instead of single channels.

p15, figure 6: the minimum wavelength results 934nm but following the plot, other wavelengths such as 930-935 could be also possible. Please state the specific reason to select 934nm. Is it based on the absolute differences between the different techniques? As this plot is specific for the two year database analysed, perhaps channel 932 or 933nm could be more robust as it is situated on the center of the optimum region (however I acknowledge that little effect is expected). –

In the monochromatic approach 934 and 935nm channels statistics were almost as good as 946nm and 946nm band was selected for consistency with WMO recommendations and filter photometers. Following that we wanted the spectral approach to have windows that include all these bands. But still as shown in theoretical spectras the higher absorption is in the 944-946nm region, so windows not including that have serious drop in the quality of the final retrieval. That is the reason that we select to move only the lower limit of the window and always have this region included.

The most unexpected behaviour is that CIMEL has better agreement in a spectral region including a significant part outside its measuring band (at 932-946nm).
Reason for selecting 934nm as the lower limit is that “average” better for all comparisons (CIMEL is better in the wider window, MWP and RADIOSONDE agreed best at 936-946nm and GPS is practically equal in any selection). So the selection of a different window would slightly alter accordingly the statistics of each comparison. The corresponding sentence in the manuscript has been restated to clarify the selection.

Tables: please include the units in all the correspondent columns.

Units are now stated in all columns.

Referee 3

P3, l. 15: Actually, AERONET has more than four hundred sites around the world.

The sentence has been restated

P3, l. 26: "Izaña Atmospheric Observatory, Tenerife, Spain" seems to be in different font type.

Fonts changed

P4, l. 16: Add space after (MOL-RAO).

Added,

P5, l. 23: Cimel performs measurements at nine bandpass filters, and retrieves AOD at eight nominal wavelengths (340-1640nm with the exception of 940nm).

The sentence has been restated.

P5, l. 23: 1064nm>1640nm

Corrected.

P5, l.27: Please clarify what you mean by "retrieve it" in this sentence.

The sentence has been restated to be clear that it refers to IWV retrieval and not FWHM.

P6, l. 25: Add space after 2.4.

Added

P8, l. 3: quaiity>quality

Corrected

P8, l.19: Section 3.2.

Added

P10, l. 10: The authors stated they used mid-latitude atmosphere to model T_w. What season have you selected for your simulations? Do you expect a change in three wavelength dependent coefficients (a, b and c) as a result of the seasonal change inT_w, as was found by Campanelli et al. (2014) or Schmid et al. (1996)?

All the runs were made with summer mid latitude model. Ingold et al. (2000) showed that the most important parameter that significantly alter retrievals is altitude.

Campanelli et al (2014) found an important seasonal variability of the coefficients (although retrieved without RTM) and in their newer (Campanelli et al, 2018) study they developed a method to recalculate them in daily basis almost in daily basis, using GPS reference. In our case of RTM calculations and the aim of having a stand-alone method, we considered the vertical profiles of the atmosphere, which alter the coefficients as unkwown and just used one set of runs. As in Ingold et al. (2000) this choice adds an uncertainty of ~0.05% to the coefficients, which is inisignificant in our uncertainty budget calculation in section 4 of the manuscript.

P18, l. 6: The reference Smirnov et al. (2000) should be used in the next sentence,where the AERONET cloud screening is presented.

Reference has been added to the appropriate sentence.

P19, l. 6: Figure 8>Figure 9

Figure numbers have been updated an corrected.

P20, l. 9: statics>statistics

Corrected

P20, l. 14: Is sigma defined as the standard deviation somewhere in the text?

Standard deviation is defined now defined in the beginning of the results section, alongside with a clarification of the differences calculated.

P21, l. 18: figure 11>Figure 11

Figure numbers have been updated an corrected.

Water Vapor Retrieval using the Precision Solar Spectroradiometer

Raptis Panagiotis-Ioannis[1,2], Kazadzis Stelios[1], Gröbner Julian[1], Kouremeti Natalia[1], Doppler Lionel[3] , Becker Ralf[3] , Helmis Constantinos[2]

[1]*Physikalisch-Meteorologisches Observatorium Davos-World Radiation Center (PMOD-WRC), Davos, Switzerland*

[2]*University of Athens, Department of Physics, Athens, Greece*

[3]*Deutscher Wetterdienst, Meteorologisches Observatorium Lindenberg – Richard Assmann Observatorium (DWD, MOL-RAO), Lindenberg (Tauche), Germany*

Abstract.

The Precision Solar SpectroRadiometer (PSR) is a new spectroradiometer developed at Physikalisch-Meteorologisches Observatorium Davos-World Radiation Center (PMOD-WRC), Davos, measuring Direct Solar Irradiance at the surface, in the 300-1020 nm spectral range at high temporal resolution. The purpose of this work is to investigate the instrument's potential of retrieving Integrated Water Vapor (IWV) using its spectral measurements. Two different approaches were developed in order to retrieve IWV, the first one using single channel/wavelength measurements, following a theoretical water vapor high absorption wavelength, and the second one using direct sun irradiance integrated at a certain spectral region. IWV results have been validated using a 2-year dataset, consisting of an AERONET sun-photometer Cimel CE318, a Global Positioning System (GPS), a Microwave Radiometer Profiler (MWP) and radiosonde retrievals recorded at Meteorological Observatorium Lindenberg, Germany. For the monochromatic approach, better agreement with retrievals from other methods/instruments was achieved using the 946nm channel, while for the spectral approach using the 934-948 nm window. Compared to other instruments' retrievals, the monochromatic approach leads to mean relative differences up to 3.3% with the coefficient of determination (R^2) being in the region of 0.87-0.95, while for the spectral

approach mean relative differences up to 0.7% were recorded with R^2 in the region of 0.96-0.98. Uncertainties related to IWV retrieval methods were investigated and found to be less than 0.28cm for both methods. Absolute IWV deviations of differences between PSR and other instruments were determined the range of 0.08-0.30 cm and only in extreme cases would reach up to 15%.

1.Introduction

Water Vapor is a very important component of the thermodynamic state of the atmosphere (Hartman et, al 2013), being a greenhouse gas with relatively high concentrations. The quantity of water in the vapor state depends on temperature. So, from a climate change perspective, it is considered as a feedback agent (Soden and Hled, 2006). Also, it is an important component of the hydrological cycle and estimations of it are used in meteorological forecast models (eg. Hong et al., 2015, Bock et al., 2016). Finally, a robust estimation is needed to study microphysical processes that lead to the formation of clouds and determine their composition (water droplets or ice crystals) as well as the statistical shape and size of these components (Reichard et al., 1996, Yu et al., 2014).

IWV in the vertical atmospheric column is a very common variable in meteorological and climatological studies. It is defined as the height that water would stand if completely condensed and collected in a vessel of the same unit cross section (American Meteorological Society, 2015). Monitoring of water vapor in the atmosphere has been performed through radiosondes and provided through measurements of vertical profiles of humidity. These measurements are limited to relatively infrequent (radiosonde) launches; thus, during the last decades there have been developed methods to retrieve IWV from other devices:

- Continuous monitoring of IWV is established through Global Positioning System (GPS) satellite observations (Bevis et al., 1992), which could be used to retrieve IWV anywhere in the globe at relatively high temporal frequencies. The theoretical basis for these measurement is that delays in the signals emitted by GPS satellites are caused by the amount of water in the atmosphere, and through proper calibration, such delays could be expressed as function of the IWV. Thus, as long as there are ground based GPS receivers, after the appropriate post-processing of the received signals, IWV can be retrieved.

- Microwave Radiometer Profilers (MWP) measure the emitted microwave radiation of the atmosphere and retrieve water vapor vertical profiles and then IWV, providing continuous data at very high frequencies under all weather conditions (e.g. Güldner and Spankuch, 2001, Güldner, 2013). These instruments provide very high accuracy but are not very common.
- Measurements from sun-photometers (eg CIMEL, PREDE-POM, MFR) have also been used to calculate water vapor transmittance and, thus, estimate IWV. Filter radiometer recordings in the spectral region around water vapor absorption bands, in the near infrared region, are used to calculate this quantity (Halthore et al., 1997, Campanelli et al., 2018, Nyeki et al., 2005). The World Meteorological Organization (WMO) recommends the use of spectral windows centered around 719, 817 and 946 nm, though the most frequently used is the 946 nm bandpass, which Ingold et al. (2000), showed that provides the most robust results.

Global networks of deployed sun-photometric devices are capable of providing IWV time series. The AErosol RObotic NETwork (AERONET) retrieves IWV at more than five hundred stations around the globe since the 1990's (Holben et al. 1998, https://aeronet.gsfc.nasa.gov/) using the Cimel instrument. Other sun-photometers such as the Precision Filter Radiometers (PFR) (Nyeki et al., 2005) have also been used by the Global Atmosphere Watch (GAW) WMO program to monitor IWV. Furthermore, the SKYNET radiometer network (details on: http://atmos2.cr.chiba-u.jp/skynet/) also retrieves IWV using Prede-POM sunphotometers at many stations (Campanelli et al., 2012, 2014). Finally, national networks of sunphotometers are installed and operating in some countries also provide Integrated Water Vapor (IWV) retrievals, eg. China Aerosol Remote Sensing NETwork (CARSNET) is using the 936nm channel to provide IWV (Che et al., 2016).

Schneider et al. (2010) provided a very detailed comparison of different instrument retrievals over a 4-year data set recorded at Izaña Atmospheric Observatory, Tenerife, Spain. They found that MWP is the most precise technique and, in addition, it is independent of weather conditions, while sun-photometric retrievals were limited by cloudy and biased by dry/humid atmospheres, and GPS retrieved IWV showed deviations at lower IWV values. Deviations were also recorded when compared to radiosondes, which was explained by the difference in air masses and time scales among radiosondes and other IWV retrievals.

Deleted: one

Technological advances of the recent years have made feasible the manufacturing of operational spectral sun-photometers for environmental monitoring. The Precision Solar Spectroradiometer (PSR), designed and manufactured at PMOD/WRC , Davos, Switzerland, is one of the most accurate instruments of this class (Gröbner et al., 2012) . In this study we have developed tools to retrieve IWV using PSR recordings, adopting two different approaches; one using single wavelength channels and another retrieving from a wider spectral region, the latter being impossible with filter radiometers. Retrievals in different channels and spectral windows in the water vapor absorbing region of near infrared spectrum were evaluated and selected. Both methods were applied to a 2-year long PSR dataset at the German Meteorological Service (Deutscher Wetterdienst, DWD) site in Lindenberg, Germany and results have been compared with sun-photometric (CIMEL), GPS, radiosonde and MWP IWV datasets from the same station. Present study presents the technical details of all instrumentation used, describes all the details of the development of this two methodological approaches and estimates the uncertainties linked to them and finally all the comparisons for the 2 year dataset are reported.

2.Instrumentation

Methodologies for retrieving IWV were applied to PSR measurements *at Meteorologisches Observatorium Lindenberg – Richard Assmann Observatorium* (MOL-RAO) from the German Meteorological Service "Deutscher Wetterdienst" (DWD) in Lindenberg (Tauche), in the North-East Germany (52° 12′ N, 14° 7′ E), where a 2-year long PSR dataset is available (May 2014- April 2016). MOL-RAO is a supersite for measurements of aerology and radiation, thus it provides a variety of collocated measurements that could be used for validation. MOL-RAO is exclusively devoted to instrumental measurements of the atmosphere and a numerous technical staff guarantees daily maintenance of the instruments. All instruments and corresponding techniques are described below. Sunshine at the area ranges from 55 hours/month at December to 256 hours/month during summer months on average; also, rain is recorded almost for 1/3 of days during all 12 months (Beyrich and Adam, 2005). Minimum solar zenith angle (SZA) reaches 30º during summer months while during winter it is over 70º. AOD is generally very low in the area, with maximum mean monthly values of 0.25 an 0.27 during June and July.

Deleted:

2.1 PSR

A new generation of solar spectroradiometer, the Precision Solar Spectroradiometer (PSR) (Figure1) , is being developed at PMOD/WRC in order to eventually replace current filter sun-photometers. It is based on a grating monochromator of stabilized temperature with a 1024 pixel Hamamatsu diode-array detector, operating in a hermetically sealed nitrogen-flushed enclosure. The spectroradiometer is designed to measure the solar spectrum within the 300 to 1020 nm wavelength range with an average step of ~0.7nm and spectral resolution from 1.5 nm to 6 nm (full width at half maximum, depending on the measured wavelength) (Kouremeti and Gröbner, 2012). The design benefits from the experience gained from successive generations of the successful Precision Filter Radiometers (PFR), including: an in-built solar pointing sensor, an ambient pressure sensor and temperature sensors to provide routine quality control information, which allows autonomous operation at remote sites with state-of-the-art data exchange via Ethernet interfaces. The PSR used in this study is the PSR#006, which is installed on the MOL-RAO site. This instrument has been calibrated at PMOD/WRC using a 1000 W transfer standard lamp source, in May 2014 and October 2015. A comparison between the two calibrations showed relative differences less than 1% for most spectral channels and more than 2% only in the region above 980nm (Kouremeti et al. , 2015). Moreover, stray light corrections have been applied and absolute direct and global (horizontal) Irradiance time series are available for all 1024 available channels (Gröbner et al., 2014). The cycle of routine measurements during this period was in a set of 5 Direct solar Irradiance and 5 dark current measurements and average values for each pixel was saved at 1minute resolution. An evaluation of AOD retrievals from PSR have been performed during the 4th Filter Radiometer Comparison (WMO, 2016, Kazadzis et al., 2018).

Formatted: Superscript

Formatted: English (UK)

Figure 1. *PSR#004 and PSR#006 installed on a sun tracking device at MOL-RAO,*

Formatted: Font:Italic

Formatted: Font:Italic

2.2 CIMEL Sun-photometer

The CIMEL sun-photometer is a filter radiometer developed by Cimel Electronics (Paris, France), which performs direct sun and sky radiance measurements. These measurements are processed centrally and are widely available through Aerosol Robotic Network (AERONET) (Holben et al., 1998). Measurements are performed at nine bandpass filters between 340 and 1640 nm (8 of them dedicated to AOD retrieving and one used for IWV). Direct measurements are performed usually every 10-15 minutes. Direct sun measurements at 940 nm are used to retrieve IWV. At this channel the Full Width Half Maximum is 10nm, (Schmid et al., 2001) which means that the solar signal recorded represents a relatively wide spectral region. The method used to retrieve IWV is described in detail in Smirnov et al. (2004). The principle of this method is to calculate a two constants' fit, using radiative transfer model calculationsin order to retrieve IWV from the transmittance recorded at 940 nm. The precision of this retrieval was investigated by Alexandrov et al. (2009) who showed an error in the region of 0.05-0.18cm depending on the amount of IWV.

Deleted: eight

Deleted: 1064

Deleted: it

The CIMEL Level 2 AOD data for MOL-RAO has been directly downloaded from AERONET website (https://aeronet.gsfc.nasa.gov/). During the 2 years of this study, the station has been equipped with three different instruments:

- Cimel CE318N, #787
- Cimel CE318N, #873 supplying #787 during its AERONET calibration
- Cimel CE318T ("Triple") since October 2015, instrument of higher temporal resolution (~ 1 minute)

2.3 Global Positioning System

GPS is a space based system that uses the signal transmitted from specific satellite instrumentation in order to define the geolocation of ground based receivers. The signal delays could be separated into dry (dependent on dry air gases) and wet (water vapor) component. Although the biggest fraction of the delay is caused by the dry component, it is estimated by hydrostatic equations, using the surface pressure, and subtracting it from the total delay. This is considered a very accurate retrieval of the wet component, to which IWV is directly proportional (Bevis et al, 1992). Wang et al. (2007) showed that the random error of GPS IWV retrievals is in the order of 0.7 mm. GPS IWV retrievals are very valuable, since this method could be applied to any receiver and obtain a very reliable and dense dataset of frequent observations, both for daytime and night time, without being affected by cloud conditions. Differences among GPS and sun-photometric retrievals are expected, as different optical paths are used in each case and different air masses are detected: GPS path is a quasi-random path depending on the position of the satellites while the sun-photometer path is defined by the sun-instrument's relative positions.

2.4 Microwave Radiometer Profiler

At MOL-RAO, a 22-channel MWP, MP-3000A /Radiometrics (Ware et al., 2003) provides vertical temperature and humidity profiles. In principle, observations from these instruments are based on recording the down-welling thermal emission of the atmosphere in the region between 22 and 30 GHz, using a zenith sky looking sensor. A full description of the Water Vapor retrieval methodology of MWP could be found at Westwater et al. (2005). Cadeddu et al. (2013) have estimated the uncertainty of this technique in the order of 5% for IWV less than 10mm.

2.5 Meteorological Radiosonde

Meteorological radiosondes (RS) are launched in many places around the world, recording vertical profiles of various meteorological variables (Temperature, Wind Speed, Humidity etc). Water Vapor profiles provided by the soundings can be used to calculate IWV. This is the most objective approach for validating ground based remote sensing techniques, since water vapor is measured in-situ during the ascending procedure. Uncertainty for IWV retrieval in this approach is introduced by the nature of the method, as the total ascending of a radiosonde to stratosphere takes approximately an hour and also the path of the radiosonde in the atmosphere is determined by winds; thus, it is not directly comparable to sun-photometric estimations, which retrieve water vapor on the sun-point of observation optical path. High uncertainties -up to 20%- for relative humidity, caused by warming due to sunlight and thermal lag, have been reported (Pratt, 1985). Also, studies have reported differences due to the use of different sensors (e.g. Soden and Lanzante 1996). Vaisalla RS92 radiosondes are used in this study for which an uncertainty in the order of 5% for the RH (Relative Humidity) measurements, during daytime in the Troposphere, has been reported (Miloshevich et al.,2009). Radiosondes from MOL-RAO are launched 4 times per day (00h, 06h, 12h, 18h UTC). So, for this study 1-3 daytime soundings, per day, can be used, depending on the season. Corrections, as suggested by Vömel et al. (2007) for the dependence of the humidity sensor on temperature and radiation, were applied.

3. Methodology

In the near infrared measuring spectral region of PSR the most important water absorption has been found in the 700-1000 nm wavelength region. Figure 2 shows the transmittance from Rayleigh scattering, aerosols and IWV, as calculated by the MODerate resolution atmospheric TRANsmisson Radiative Transfer Model (MODTRAN RTM) (Berk et al., 1987, Berk et al., 1999). Aerosols direct effect on irradiance is measured through Aerosol Optical Depth (AOD) which is the integrated extinction coefficient on vertical column due to aerosols. Spectral variation of AOD at different wavelengths is measured through Ångström Exponent. For the example on figure 2, Ångström Exponent equal to 1.5 was considered and aerosol of AOD 0.1 and 0.2. Inclination of aerosol transmittance lines is proportional to Ångström Exponent and higher AOD will lead to lower absolute values. WMO (2004) recommends 719, 817 and 946 nm central wavelengths to retrieve IWV, which appears as significant drops in the solar transmittance spectra in Figure 2. Ingold et al. (2000) investigated the quality of the

Deleted: 1

Deleted: 1

Deleted: 1

retrievals at these wavelengths and found that the one at 946 nm is the most robust, which could be translated as the wavelength range with the strongest absorption of IWV. Considering that absorption of water vapor is higher in the 910-950 nm region, all calculations were performed for PSR channels in the spectral range.

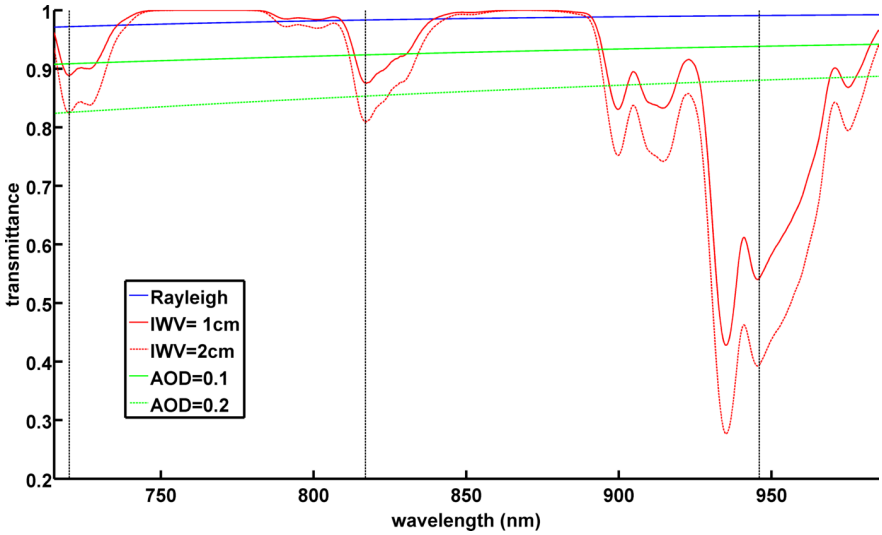

Figure 2, *Transmittance of Water Vapor, Aerosols and Rayleigh scattering in the spectral region 700-1000 nm, calculated using MODTRAN set at 0.1 nm resolution, at SZA=0º IWV=1cm, IWV=2cm and AOD=0.1 and AOD=0.2 at 700nm using an Ångström Exponent of 1.5. Black vertical dotted lines represent WMO recommendations for IWV retrieval.*

Deleted: 1

3.1 Monochromatic Approach

The methodology in use is described in detail by Ingold et al. (2000) and it is the most common procedure to calculate IWV for sun-photometric devices using individual wavelength (filter) measurements. It is labeled as monochromatic in contrast to the second approach presented in Section 3.2, although it is calculated for a spectral region defined by the instrument's slit function or the limits of its bandpass filter.

The first step of the procedure is to calculate the Water Vapor transmittance T_w in the spectral window of use and afterwards to develop empirical formulas using RTM calculations to determine the IWV from the calculated transmittance.

For specific spectral regions in the near infrared, where absorption of dominant trace gases can be considered negligible, we can express the transmittance of the Atmosphere (T_{atmo}) as follows:

$$T_{atmo} = \frac{I_\lambda}{I_{0,\lambda}} \qquad (1)$$

where I_λ is the recorded spectral irradiance at wavelength λ (in $Wm^{-2}nm^{-1}$) and $I_{o,\lambda}$ is the value of the solar irradiance at the top of the atmosphere at the same wavelength.

We can express the Beer-Lambert law (Swinehart, 1962) ith respect to water vapor transmittance as follows:

Deleted: w

$$T_{atmo} = e^{(-m_{ray}\tau_{ray,\lambda} - m_a\tau_{a,\lambda})} * T_w \qquad (2)$$

Deleted: →

$$T_w = \frac{I_\lambda e^{(m_{ray}\tau_{ray,\lambda} + m_a\tau_{a,\lambda})}}{I_{0,\lambda}} \qquad (3)$$

where T_w is the transmittance of water vapor, τ_{ray} is the Rayleigh scattering optical depth, τ_a is the aerosol optical depth (AOD), m is the relative optical air mass of aerosol and Rayleigh scattering accordingly. For the Rayleigh scattering cross-section we have used the formula found at Bodhaine et al. (1999).

Also, for $I_{0\lambda}$ we have used extraterrestrial values calculated for each of the PSR wavelengths measured as presented by Gröbner et. al. (2017a, 2017b). Spectral AODs were calculated using the Beer-Lambert law and the above extraterrestrial solar spectrum (Kouremeti and Gröbner, 2012). For calculating AOD at the wavelengths in the 920-950nm region, where direct sun measurements are affected by water vapor, we have applied a least square quadratic spectral extrapolation, using ln(AOD) as function of ln(wavelength) and the PSR AODs at 500 - 865 nm following Eck et al. (1999) suggestion for AERONET retrievals.

In order to convert T_w into IWV we have used the three-parameter expression found in Ingold et al. (2000):

$$T_w = ce^{-a\chi^b} \qquad (4)$$

where

$$\chi = \frac{u\, m_w}{u_0} \qquad (5)$$

with u_o = 10 kg/m^2 , u representing IWV, m_w as the H_2O air mass and *a,b,c* the three wavelength dependent coefficients. At this step the coefficients of equation (4) can be estimated. For that purpose, we have used MODTRAN multiple runs for solar zenith angle (SZA) in the region of 0º to 85º with steps of 2.5º. We have used the mid-latitude built in model atmosphere, in the spectral region 0.7 to 1.0 µm and IWV from 0 to 40 mm with steps of 2 mm for site elevation set at 110m (MOL-RAO). The modeled spectra were convolved by the spectrally dependent instrument slit function in order to derive comparable (model-PSR) results. Then T_w retrieved from the output spectra was calculated as a function of Slant Water Vapor Path (m_w*u), and a fit of these values is used to estimate the coefficients (*a, b, c*) of equation (4). This procedure was repeated for all PSR channels in the whole spectral region of 900-950 nm. In figure 3, we present these fits for wavelengths 935.5 and 946 nm. Fits for wavelengths lower than 926 nm were unsatisfactory (R^2<0.7), suggesting that a different parameterization should be used in this area instead of equation (4).

Deleted: 2

After determining the coefficients *a,b,c* , equations could be solved in order to calculate the IWV :

$$IWV = \frac{1}{m_w}\left(\frac{ln\left(T_w/_c\right)}{-a}\right)^{1/b} \qquad (6)$$

Thus, IWV now depends only on T_w and air mass, although the coefficients depend on the altitude of the measurement site; so, different RTM runs are needed for each installation.

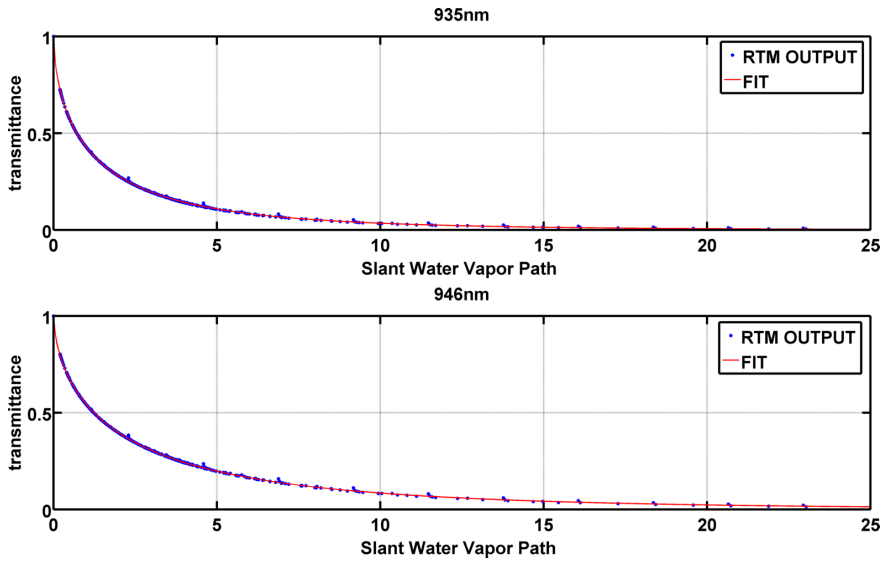

Figure 3, *Transmittance of IWV versus Slant Water Vapor Path (m_w*u) calculated by MODTRAN, and three-parameters expression fit for 935 and 946nm bandpasses.*

In order to test the above methodology, we have retrieved IWV on September 30th , 2015, for each PSR channel in the 920-950 nm region separately, after calculating wavelength dependent a, b, and c coefficients. Also, aerosol and Rayleigh transmissions were calculated separately for each wavelength. The standard deviation of the residuals retrieved from different wavelengths is 0.11. The IWV retrievals at 946 and 935.5 nm have the smallest deviations compared to the GPS and CIMEL retrievals, because at these wavelengths the absorption due to water vapor absorption is higher. At these two wavelengths, the agreement with CIMEL measurements is very good, with correlations (expressed as the R^2 coefficient) of 0.94 and 0.93 respectively. The lowest R^2 is found for wavelengths shorter than 928 nm which is in the order of 0.6. At figure 4 the mean IWV from all wavelengths for one day (30 September 2015) is presented as an example, alongside with the standard deviation of all monochromatic retrievals and retrievals at 946 nm are presented as reference. The standard deviation of the residuals retrieved from different wavelengths is 0.11. Following WMO guidelines, we decided to use retrievals at 946 nm for this study and the monochromatic approach.

Deleted: 2

Deleted: . An average value of all wavelengths in the regions 920-948nm is shown in Figure 3 for one day alongside with GPS IWV retrievals

Deleted: 3

Deleted: .

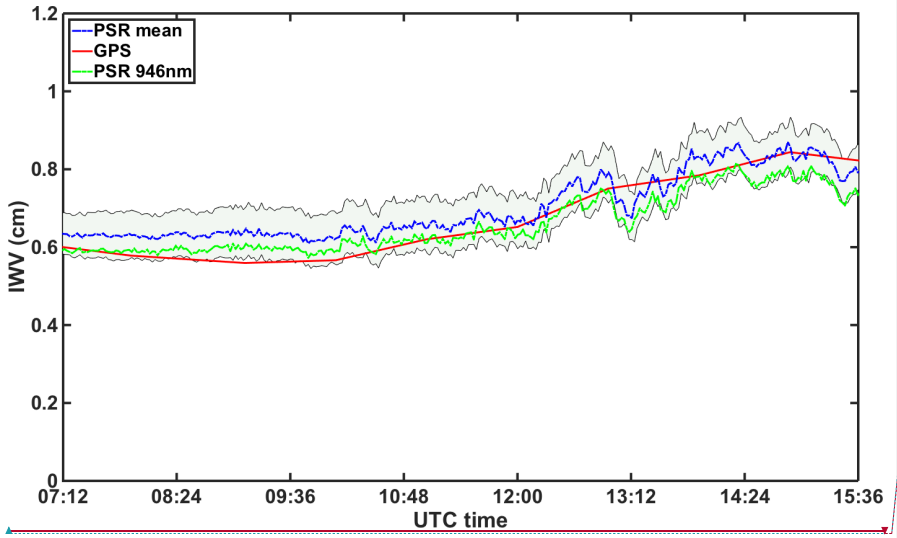

Figure 4, *Retrievals of monochromatic approach on 30th September 2015 at various wavelengths. Average IWV retrieved using the monochromatic approach at different wavelengths represented by blue line; the shaded area represents the standard deviation (1σ) of retrievals at different wavelengths, green line represent retrievals at suggested 946 nm and the red curve represents the IWV retrieved from GPS.*

3.2 IWV retrieval using integrated spectral windows

In order to benefit from the high resolution spectral measurements available from the PSR we developed a method that uses direct sun integrated irradiances for a spectral window in contrast to individual/single wavelengths as previously described. This methodology is expected to improve the IWV retrieval, since the large variability found in the IWV retrievals at different wavelengths suggests that an approach that combines different wavelengths could possibly be more accurate. Figure 5 shows two theoretical spectra in the region of 700-1000 nm (calculated using MODTRAN), at SZA=0º with no aerosol load and with 0 and 2 cm of IWV respectively. In this approach we have used the transmittance of the whole spectral window, and then equation (3) can be written as follows:

$$T_{w,\Delta\lambda} = \frac{\int_{\lambda_1}^{\lambda_2} \frac{I(\lambda)\exp\left(m_{ray}\tau_{ray}(\lambda)+m_a\tau_a(\lambda)\right)}{I_0(\lambda)} d\lambda}{\Delta\lambda} \qquad (7)$$

Formatted: Font:Bold

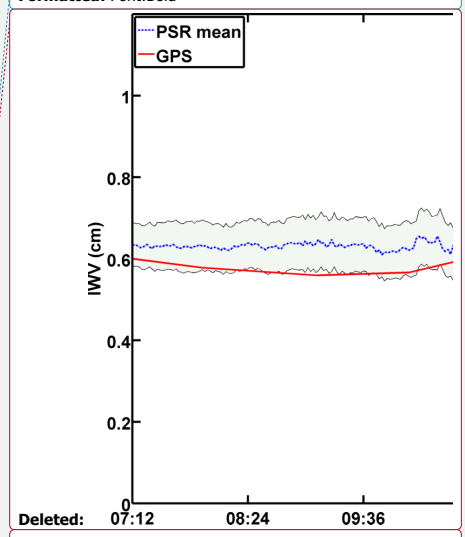

Deleted:

Deleted: 3

Deleted: 4

Where λ_1 and λ_2 are the area wavelength limits, and $\Delta\lambda=\lambda_2-\lambda_1$.

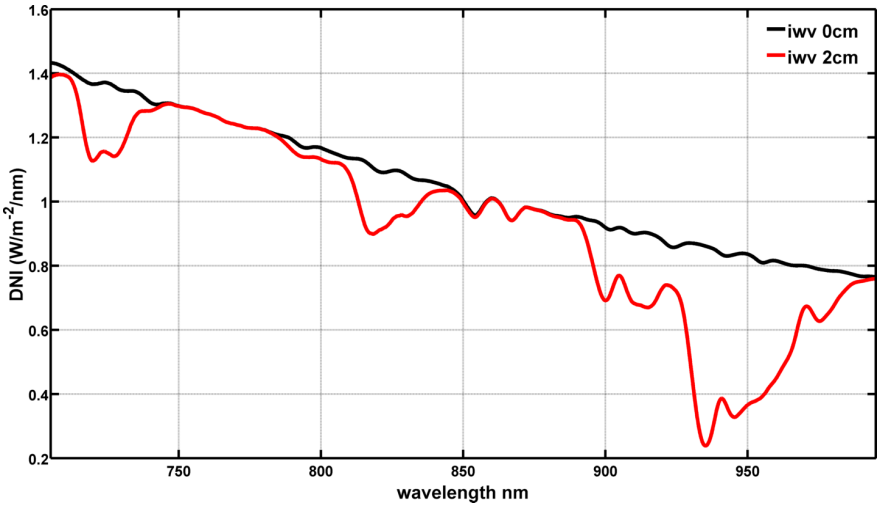

Figure 5, *Calculated Spectra of Direct Solar Irradiance, at SZA=0º with AOD=0 and IWV=0 cm (black) and 2 cm (red), as calculated from MODTRAN 5.2.1 RTM.*

Deleted: 4

A similar methodology for converting transmittance to IWV, as in the monochromatic approach described above is applied again in order to calculate a third order polynomial function, valid for the wide spectral region. The same MODTRAN outputs were used as in the monochromatic approach but integrated over each spectral window, and the coefficients for equation (4) were calculated accordingly. Calculations have been performed for spectral windows with variable wavelength limits. An investigation on the selection of spectral window has been performed because, as monochromatic retrievals suggested (figure 4), the IWV calculation depends on the wavelength region in use. This investigation was made by changing the window, keeping the upper limit fixed at 948 nm and having the lower one varying between 930 to 946 nm with a step of 1 nm. This selection was made based on the water vapor absorption features as shown in Figure 5, so that the spectral window always includes the high absorption region of 943-947 nm. Longer than 947 nm wavelengths were avoided as there were higher uncertainties in the PSR calibration (Kouremeti et al., 2015, Gröbner et al., 2017). As demonstrated in Figure 6 (for the 934 - 948 nm window), fitting of the 3-parameter equation had results of similar statistics with the monochromatic approach

Deleted: 3

Deleted: 4

Deleted: 4

in that region. Residuals from fitting at this window are at average at 0.007 but there are also some up to 0.04. So, for each spectral window a new 3-parameter function is calculated.

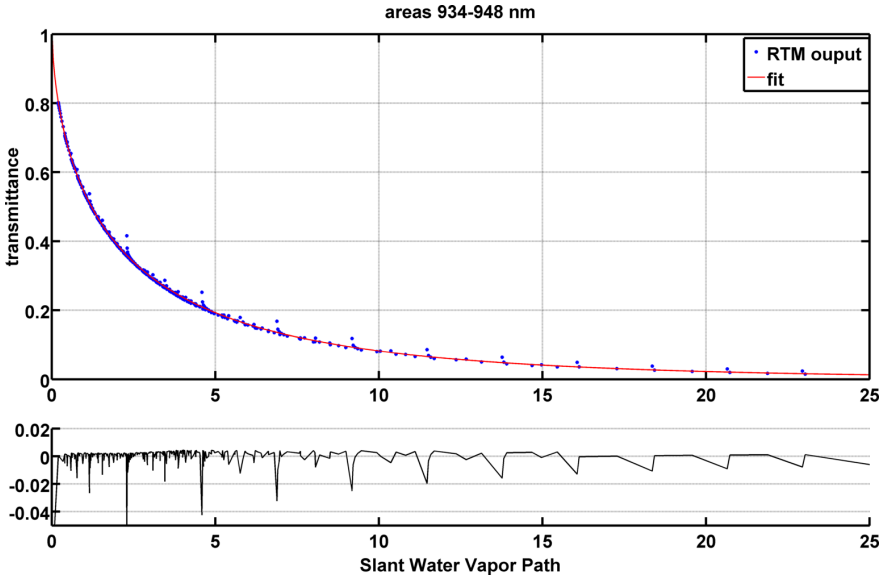

Figure 6, *Integrated Transmittance of IWV in the 934-948 nm window versus Slant Water Vapor Path (m_w*u) calculated by MODTRAN, and Third order polynomial fit.*

Deleted: 5

In figure 7 results from different spectral windows have been compared to other instruments' retrievals for the whole MOL-RAO dataset. The coefficient of determination R^2 has been used to evaluate the performance of the spectral approach at different spectral windows, and was calculated as below:

Deleted: 6

$$R^2 = 1 - \frac{\sum_i (y_i - f_i)^2}{\sum_i (y_i - \langle y \rangle)^2} \qquad (8)$$

where y_i are the IWV values from the other instruments (CIMEL, MW, GPS, RS), <y> is the average of those values and f_i are the IWV values from PSR.

Horizontal axis of figure 7 represents the lower limit of the spectral window, the higher being always fixed at 948 nm. The aim of this step is to find out which spectral window produces the more robust IWV retrieval results. These comparisons suggest that different spectral windows selection lead to different coefficients of determination for IWV retrieval compared with different instruments. However, results converge to defining a lower wavelength limit

Deleted: 6

between 932 and 936 nm, that will provide the best agreement for all the comparisons. The window 934-948 nm was selected to be used for further analysis, as a median of the above mention area.

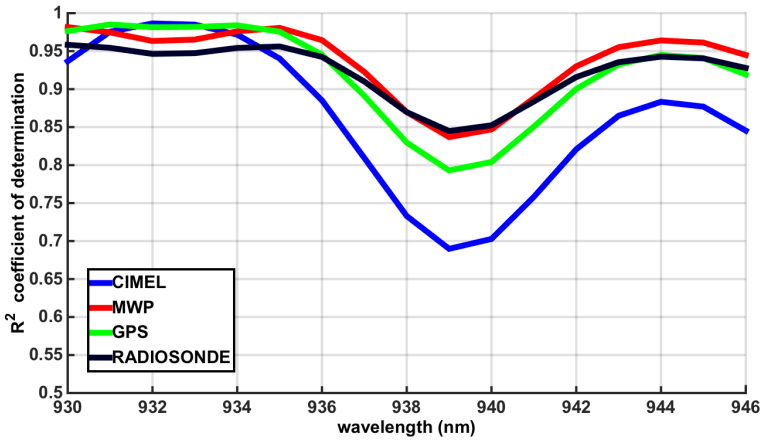

Figure 7, *IWV retrievals from PSR using spectral approach with different spectral windows, using fixed upper boundary at 946 nm and moving lower boundary at x axis, compared to synchronous ones of CIMEL, GPS, MWP and radiosonde, for the full 2-year measuring period.*

It is interesting to observe different R^2 of the PSR IWV retrievals as compared using different instruments. Especially the fact that by minimizing the spectral window the R^2s decrease showing a minimum of at window 939-946 nm. For this particular range all R^2s are below 0.85 with the one of CIMEL-PSR showing a minimum. The differences observed when comparing the PSR using different instruments can be partly explained based on the results of section 5.

4. Uncertainty budget of IWV retrievals

Uncertainty estimation of the IWV retrieval is very crucial for evaluating our comparison results. Beginning from equations (3) and (7) and the calculations of *Tw*, errors as introduced

Formatted: Font:Bold

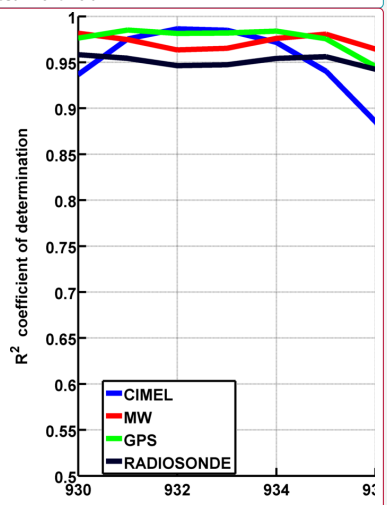

Deleted:

Deleted: 6

Deleted: comparing

from each variable are estimated and their propagation to the total uncertainty of IWV retrieval is calculated.

$$T_w = \frac{I_\lambda e^{(m_{ray}\tau_{ray,\lambda}+m_a\tau_{a,\lambda})}}{I_{0,\lambda}} \quad (3)$$

From equation (3), the term that introduces the higher uncertainty in the retrieval of the IWV through the use of Beer-Lamber law is the AOD. A benefit from the methodology applied in this case is that the same set of I_o are used for calculating T_w and AOD, and so errors related to the determination of I_o do not propagate in the calculations. PSR AOD retrievals at 865 nm have been found in accordance with prototype PFR triad when compared during FRC IV, 2015 (Filter Radiometer Comparison (GAW, 2016)) with average AOD differences at 865nm less than 0.02. Also, a calibration stability study of the PSR was performed (Kouremeti et al., 2015) and showed that the instrument was stable in the 2-year dataset of MOL-RAO, demonstrating a mean difference of 0.3% with maximum of 4% in some channels. In addition, comparison with different CIMEL instruments for longer periods in all cases showed differences smaller than 0.03 at AOD at visible and near infrared wavelengths (Kouremeti and Gröbner, 2014). So, the AOD related uncertainty calculated in all studies for the PSR is in at maximum 0.03.

Rayleigh optical depths in this spectral region are very low (~0.01 for 1000 mb pressure) and the uncertainty is 1% (Teillet, 1990) and, thus, we may consider it negligible for the IWV retrieval. Air masses were calculated using the formula found in Kasten (1966), which assumes a standard vertical profile of humidity in the troposphere and introduces an error of 10% at SZA higher than 85º, due to variations in real atmospheric conditions but is negligible for SZA lower than 75º (Tomasi et al., 1998).

Coefficients a, b, c derived from fitting of MODTRAN outputs introduce an uncertainty that is related to the goodness of the calculated fit. For the monochromatic approach at 946nm, Root Mean Square Error (RMSE) is 0.0021 and for the spectral approach at window 934-948nm it is 0.0029. So, the uncertainties introduced using the empirical equation to estimate IWV from T_w is 0.2% and 0.3% for each approach accordingly, due to the fitting.

Uncertainty is also introduced by the extrapolation of AOD from the 865 nm and lower wavelength region to water absorbing wavelengths in the range of 934-948 nm. A sensitivity

analysis of the IWV retrieval in respect to fluctuations in AOD caused by the uncertainty of AOD was performed. The uncertainty of this extrapolation was calculated to be 0.03.

Figure 8 shows the total expected uncertainty of IWV retrieval with respect to SZA, for the case of AOD=0.3 at 865 nm and the case of IWV equal to 2 cm. Highest uncertainties are expected for higher than 75° SZA, when IWV is very low or AOD very high. Very low IWV values could be found only at very dry atmospheres and even then, those are rarely below 0.2 cm. In the range of values found in the dataset of MOL-RAO (0.3 - 4.5cm), the maximum uncertainty is 0.28cm. For the 0.3 - 0.5cm values in our dataset, absolute uncertainty is calculated as 0.08-0.12 cm. Thus, the maximum expected uncertainty of the method, using PSR instruments, is found at the range of 15%, when the solar zenith angle is very high (SZA>75º) and AOD higher than 0.9.

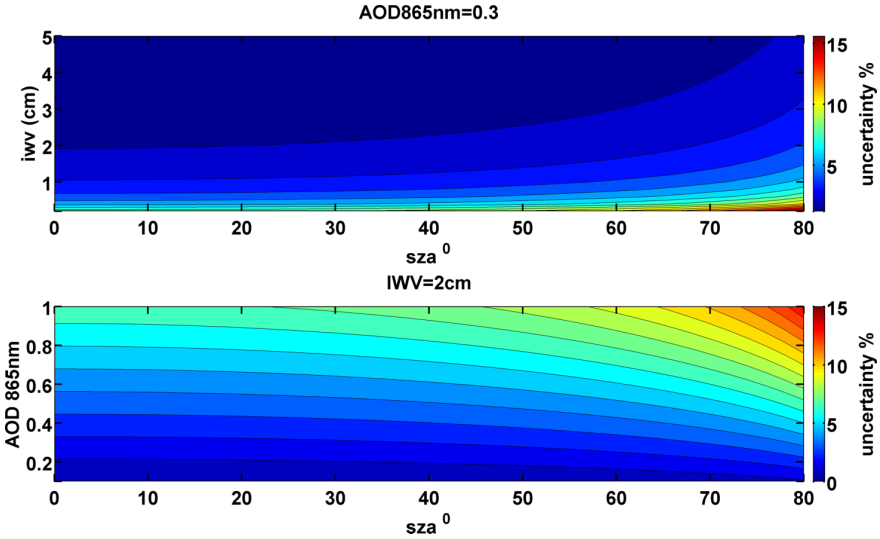

figure 8, Uncertainty (%) of *IWV retrieved using monochromatic approach at 946 nm, for various Solar Zenith Angles (º) test figure, in respect to AOD (when IWV=2cm) in upper plot, and with respect to IWV (when AOD=0.3) in lower plot.*

Deleted: 7

Deleted: 7

5. Results

In order to validate the results retrieved from both methodologies, we have used the various IWV datasets recorded at MOL-RAO. Calculations have been performed for all PSR measurements, but we have used only the ones synchronous to CIMEL level data in order to avoid cloud contamination. So indirectly the AERONET cloud screening procedure (Smirnov et al., 2000)has been used. For each CIMEL data point we have calculated the synchronous PSR value by averaging all values in a ±5 min interval. This approach produced a dataset of 3501 synchronous data points between PSR and CIMEL, 2507 between PSR and GPS and 2964 between PSR and MWP. For radiosondes, in order to have a robust coincidence criterion, we have followed the approach of Schneider et al. (2010) averaging PSR measurements for ±20 min from the time that the radiosonde reaches a 4 km height, in order to minimize spatial and temporal PSR and radiosonde measurement differences.

For all the comparisons statistics are calculated for the differences

$D_X = IWV_X - IWV_{PSR}$ (9)

where x is the corresponding instrument/method, μX is the average value for DX and

$$\sigma = \sqrt{\frac{\sum_1^N |D_{xi} - \mu_x|^2}{N-1}} \quad (10)$$

where N is the number of available, quality controlled observations.

For the monochromatic approach at 946 nm, the comparison is presented in Figure 9 and corresponding statistics in Table 1. Better agreement was found when compared to MWP retrievals, but at similar level as for the comparisons to CIMEL and to GPS retrievals. Mean absolute difference is slightly lower when compared to GPS (0.01 cm), but the spread of the differences is almost the same for CIMEL, GPS and MWP (standard deviation between 0.17 cm and 0.18 cm). Differences with CIMEL retrieval are within the CIMEL uncertainty range. It appears that PSR overestimates the IWV compared to CIMEL for IWV larger than 3 cm, which causes the different slope in the graphs. This feature is not shown in the comparison with GPS and MWP at these IWV values. Schneider et al. (2010) also observed a different behavior of CIMEL retrievals as compared to other methods, regarding dry or wet conditions in the atmosphere and linked to filter characterization errors. Radiosonde retrievals had largest deviations and more scattered differences, which is expected because of the different temporal and spatial scale of the RS retrieval. Percentiles 10-90 of the differences are also

Moved down [1]: (Smirnov et al., 2000).

Moved (insertion) [1]

Deleted: .

Formatted: Subscript

Formatted: Subscript

Formatted: Subscript

Deleted: 8

Deleted: 02

Deleted: 16

presented in table 1 and GPS, MWP and CIMEL retrievals have a spread of differences in the range of the uncertainties described for these instruments. In general RS retrievals demonstrate the most spread differences from the PSR retrievals, though the average and median are in the uncertainty range of the instruments. The high spread of the differences is explained by the random error introduced by the temporal variability of IWV in the time range averaged (±20min)and by the different paths of the sounding.

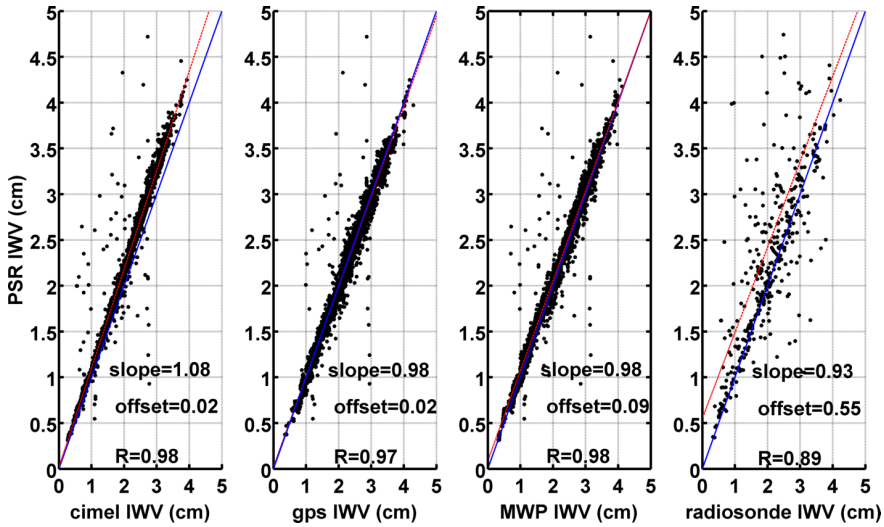

Figure 9: IWV retrievals from PSR using monochromatic approach at 946 nm compared to synchronous ones of CIMEL, GPS, MWP and radiosonde, for the full 2-years measuring period.

A histogram of relative difference of this retrieval compared to GPS is demonstrated in Figure 10. Also, IWV retrievals relative differences are shown against other parameters (AOD, SZA and IWV from GPS). A normal distribution with mean at 0.024 cm and standard deviation of 0.084 is fitted to the differences and passed the One-sample Kolmogorov-Smirnov test (Marsaglia et al., 2003). Thus 95% of the absolute differences are lower than 0.16cm. IWV differences against AOD at 865 nm show that almost all absolute relative differences higher than 0.2 cm (20%) are linked to AOD values higher than 0.5. This pattern could be connected to the larger uncertainty of AOD calculated by extrapolation at 946 nm, when AOD values are higher. Furthermore, it appears that most of the large differences appear at high SZA, but there are also some individual points showing large differences at lower SZA that could be

Deleted: 8

Deleted: 8

Deleted: higher error introduced

Deleted: the

Deleted: of AOD

Deleted: using different wavelengths

linked to AOD uncertainty. Compared to IWV retrieved from the GPS it appears that extreme differences are linked to overestimation from PSR when the absolute value is above 2 cm, and to underestimation when below , though GPS retrievals are not optimal at more dry conditions (Schneider et. al., 2010).

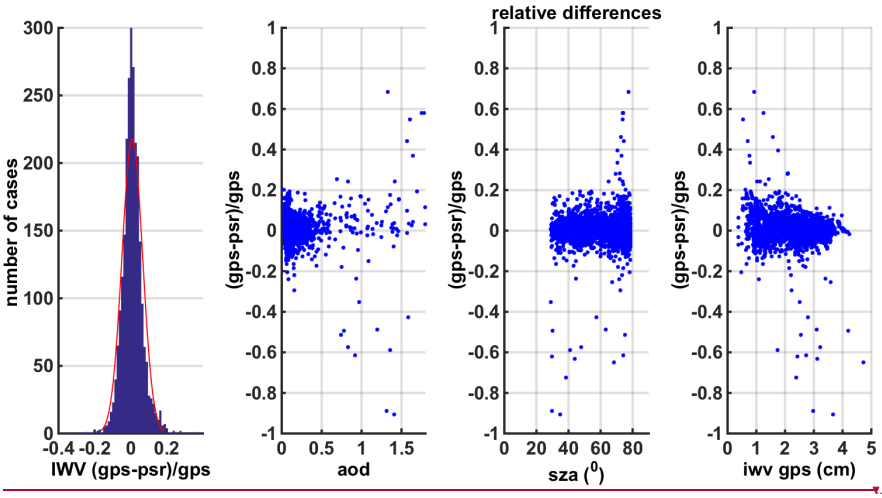

figure 10, Histogram of *relative difference among synchronous GPS and PSR retrievals – using monochromatic approach at 946 nm- and plotted against AOD (retrieved from PSR at 865 nm), solar zenith angle and IWV (retrieved from GPS).*

Comparison of the PSR spectral method with other instruments is presented in Figure 11 and corresponding statistics in Table 2. It is clear that the spread of differences with all methods is significantly lower than for the monochromatic approach. All comparisons are found with R^2 between 0.96 and 0.98. CIMEL seems to underestimate, compared to this method, but also compared with the other instruments at higher IWV values. Although the slope caused by the overestimation is still presented in this approach, the spread of the differences among CIMEL and PSR retrievals is significantly lower than any other comparison, with σ=0.07 and 10-90 percentiles of differences in a range of -0.23–0.02. Differences with GPS and MWP retrievals have the same spread and statistical behavior. Radiosonde data are in significantly better agreement with the spectral approach retrieval than with the monochromatic approach. Standard deviation of the differences is at least halved as compared to the monochromatic approach and all mean relative differences when compared to any other instrument are lower

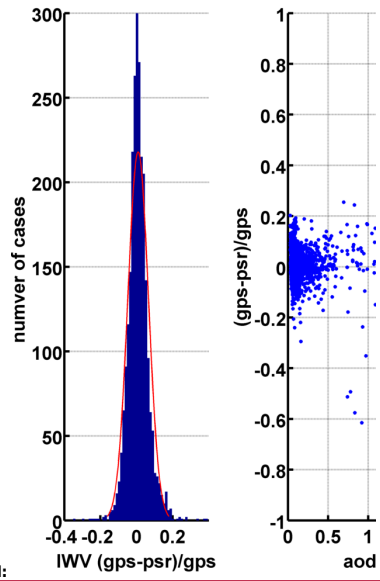

Deleted:

Deleted: 9

Deleted: ... [1]

Deleted: 10

Deleted: statics

than 0.7%. Comparison with RS' dataset has still significantly larger standard deviation than other comparisons but it is less than 1/4 of the the monochromatic approach's. Extreme values observed with the monochromatic approach are significantly reduced and the standard deviation is reduced to values from 0.07 for CIMEL to 0.18 for RS retrievals. A wider spread is observed at higher SZA, which is explained by the increase of the instrument related uncertainty at these angles.

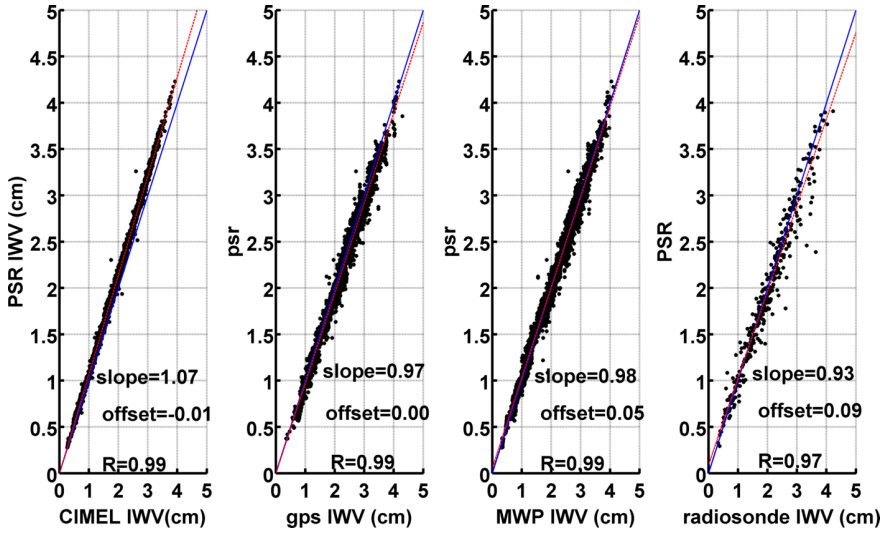

Figure 11 IWV retrievals from PSR using spectral approach at 934-948 nm region, compared to synchronous ones of CIMEL, GPS, MWP and radiosonde, for the full 2-year measuring period.

Figure 12 displays a histogram of relative differences of the spectral approach for the spectral window 934-948 nm the GPS dataset and a relative IWV comparison against: AOD at 865nm, SZA and GPS' IWV. A normal distribution with mean at 0.021cm and σ at 0.042 is fitted at the data, passed the One-sample Kolmogorov-Smirnov test (Marsaglia et al., 2003) and 95% of differences are lower than 0.08 cm. The quality of spectral retrieval shows no dependence on absolute IWV values, as the distribution of differences in Figure 12 is independent of IWV. When the IWV relative difference is shown against AOD, higher relative differences than 0.1 are more frequent for AOD lower than 0.2.

Deleted: 0

Deleted: 11

Deleted: figure

Deleted: 11

Deleted: Median differences and 10-90 percentiles.

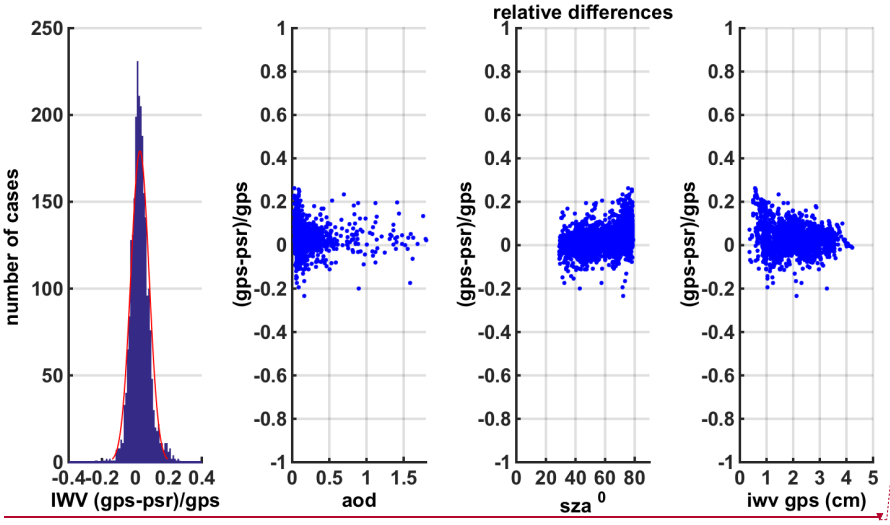

figure 12, *Relative difference among synchronous GPS and PSR retrievals – using spectral approach at 934-948nm region- plotted against (a) AOD (retrieved from PSR at 865nm), (b) solar zenith angle and (c) IWV (retrieved from GPS).*

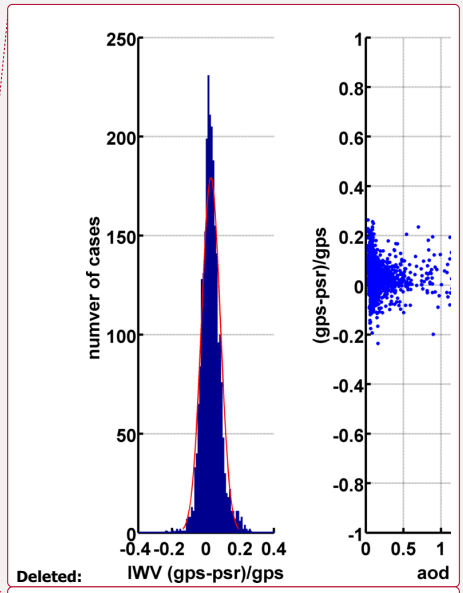

Deleted:

Deleted: 1

6. Conclusions

The aim of this study was to develop methodologies and tools in order to retrieve IWV from PSR spectral measurements. The methods which were developed can be applied to provide long term time-series of IWV using any direct sun spectroradiometer able to measure at the 930-950 spectral range.

Two approaches to retrieve IWV from PSR spectral direct solar irradiance measurements have been developed. The first one is the monochromatic approach using an individual wavelength, and the second uses a spectral window. For both methods the corresponding Water Vapor Transmittance has been retrieved from the PSR measurements, from which IWV can be calculated using a three-parameter formula following the principles of Ingold's (2000) work.

The dependence of the retrievals to other parameters has been investigated for both approaches, and found to be affected in cases of low (<0.2) AOD coincidencies. Larger

deviations were observed at high Solar Zenith Angles, which are linked to higher uncertainties in those retrievals.

Comparisons to other instruments (CIMEL, MWP) and methods (GPS, radiosondes) have been performed to select the optimum wavelength and spectral window for the IWV retrieval of the PSR. All the channels in the infrared region of 900-950 nm were tested for monochromatic approach and 946 nm bandpass was selected as giving significantly better results than other channels. For the spectral approach all possible spectral windows limits combinations were tested and the spectral window of 934-948 nm was finally chosen.

Uncertainties of the methodologies have been investigated and in more frequent atmospheric conditions have been found less than 5%, while might reach up to 15% in cases of very high AOD, very low IWV and SZA higher than 75° combined. In general, absolute uncertainty is found to be in the range of 0.08-0.3 cm.

Retrievals from a 2-year long time-series at MOL-RAO in Lindenberg, Germany showed that the monochromatic approach had differences in the order of 0.4% compared to GPS and MWP, in the order of 2.7% compared to RS, and 3.3% compared to CIMEL. 95% of differences with GPS retrievals are less than 0.15 cm.

Spectral approach's retrievals showed better agreement with other datasets, having differences of 0.7% compared to CIMEL, 0.4% compared to GPS, 0.3% compared to MWP, and 0.5% when compared to RS. Also , the differences to other retrievals were always at least half spread compared to monochromatic approach. Differences with GPS retrievals were less than 0.08cm in 95% of the dataset. Differences among the other instruments found independent of other variables, suggesting robust appliance of the method.

Overall, the accuracy of IWV retrieval is in the same order of the other well established methods and devices. The spectral approach, benefiting from the characteristics of PSR, provided statistically better results. Also, having applied the method to a 2-year dataset, indicated a stable long-term performance of the instrument, which shows that it can be used for IWV calculations. The IWV method development and assessment presented in this work provides an added value to the PSR instrument, being able to measure simultaneously spectral solar irradiance components (direct and horizontal), aerosol spectral optical properties (AOD, Angstrom Exponents) and IWV, constituting the PSR as a unique sun-photometric instrument.

7.References

Alexandrov, M.D., Schmid, B., Turner, D.D., Cairns, B., Oinas, V., Lacis, A.A., Gutman, S.I., Westwater, E.R., Smirnov, A. and Eilers, J., Columnar water vapor retrievals from multifilter rotating shadowband radiometer data. Journal of Geophysical Research: Atmospheres, 114(D2), 2009.

American Meteorological Society, Precipitable Water Vapor, Glossary of Meteorology, 2015.

Beyrich, F., and W. K. Adam, Site and Data Report for the Lindenberg Reference Site in CEOP - Phase I. Berichte des Deutschen Wetterdienstes, 230, Offenbach am Main, Germany, 55 pp, 2007.

Berk, A., Bernstein, L.S. and Robertson, D.C., MODTRAN: A moderate resolution model for LOWTRAN (No. SSI-TR-124). SPECTRAL SCIENCES INC BURLINGTON MA, 1987.

Berk, A., Anderson, G.P., Bernstein, L.S., Acharya, P.K., Dothe, H., Matthew, M.W., Adler-Golden, S.M., Chetwynd Jr, J.H., Richtsmeier, S.C., Pukall, B. and Allred, C.L., MODTRAN 4 radiative transfer modeling for atmospheric correction. In Proceedings of SPIE- The International Society for Optical Engineering (Vol. 3756, pp. 348-353),1999.

Bevis, M., S. Businger, T. A. Herring, C. Rocken, R. A. Anthes, and R. H. Ware. "GPS Meteorology: Remote Sensing of Atmospheric Water Vapor Using the Global Positioning System." Journal of Geophysical Research, Vol. 97, No. D14, , pp. 15,787-15,801, October 20, 1992

Bock, O., Bosser, P., Pacione, R., Nuret, M., Fourrié, N. and Parracho, A. : A high-quality reprocessed ground-based GPS dataset for atmospheric process studies, radiosonde and model evaluation, and reanalysis of HyMeX Special Observing 30 Period. Q.J.R. Meteorol. Soc., 142: 56–71. doi:10.1002/qj.2701, 2016.

Bodhaine, B. A., Wood, N. B., Dutton, E. G., and Slusser, J. R.: On Rayleigh optical depth calculations, J. Atmos. Ocean. Tech., 16(11), Part 2, pp 1854–1861, 1999.

Cadeddu, M. P., J. C. Liljegren, and D. D. Turner, The Atmospheric Radiation Measurement (ARM) program network of microwave radiometers: Instrumentation, data and retrievals, Atmos. Meas. Tech., 6, 2359–2372, doi:10.5194/amt-6-2359-2013, 2013.

Campanelli, M., Estellés, V., Smyth, T., Tomasi, C., Martínez- Lozano, M. P., Claxton, B., Muller, P., Pappalardo, G.,Pietruczuk, A., Shanklin, J., Colwell, S., Wrench, C., Lupi, A., Mazzola, M., Lanconelli, C., Vitale, V., Congeduti, F.,Dionisi, D., and Cacciani, M.: Monitoring of Eyjafjallajoekull volcanic aerosol by the new European SkyRad users(ESR) sun-sky radiometer network, Atmos. Environ., 48, 33–45, 2012.

Campanelli, M., Mascitelli, A., Sanò, P., Diémoz, H., Estellés, V., Federico, S., Iannarelli, A. M., Fratarcangeli, F., Mazzoni, A., Realini, E., Crespi, M., Bock, O., Martínez-Lozano, J. A., and Dietrich, S.: Precipitable water vapour content from ESR/SKYNET sun–sky radiometers: validation against GNSS/GPS and AERONET over three different sites in Europe, Atmos. Meas. Tech., 11, 81-94, https://doi.org/10.5194/amt-11-81-2018, 2018.

Campanelli, M., Nakajima, T., Khatri, P., Takamura, T., Uchiyama, A., Estellés Leal, V., Liberti, G.L. and Malvestuto, V., Retrieval of characteristic parameters for water vapour transmittance in the development of ground based sun-sky radiometric measurements of columnar water vapour. Atmospheric Measurement Techniques, 2014, num. 7, p. 1075-1087,2014.

Che, H., Gui, K., Chen, Q., Zheng, Y., Yu, J., Sun, T., Zhang, X. and Shi, G., Calibration of the 936 nm water-vapor channel for the China aerosol remote sensing NETwork (CARSNET) and the effect of the retrieval water-vapor on aerosol optical property over Beijing, China. Atmospheric Pollution Research, 7(5), pp.743-753, 2016.

Eck, T. F., Holben, B. N., Ward, D. E., Mukelabai, M. M.,Dubovik, O., Smirnov, A., Schafer, J. S., Hsu, N. C., Piketh,S. J., Queface, A., and Roux, J. L.: Variability of biomass burning aerosol optical characteristics in southern Africa duringthe SAFARI 2000 dry season campaign and a comparison of single scattering albedo estimates from radiometricmeasurements, J. Geophys. Res.-Atmos., 108, 2156–2202,doi:10.1029/2002JD002321, 2003.

Gröbner, J., Kazadzis, S., Kouremeti, N., Doppler, L., Tagirov, R. and Shapiro, A.I., February. Spectral solar variations during the eclipse of March 20th, 2015 at two European sites. In AIP Conference Proceedings (Vol. 1810, No. 1, p. 080008). AIP Publishing, 2017a.

Gröbner, J., Kröger, I., Egli, L., Hülsen, G., Riechelmann, S., and Sperfeld, P.: The high-resolution extraterrestrial solar spectrum (QASUMEFTS) determined from ground-based solar irradiance measurements, Atmos. Meas. Tech., 10, 3375-3383, https://doi.org/10.5194/amt-10-3375-2017, 2017b.

Gröbner, J., Kouremeti, N., Coulon, E., Durig, F., Gyo, M., Soder, R., Wasser, D., Spectroradiometer for Spectral Aerosol Optical Depth and Solar Irradiance Measurements, annual report PMOD/WRC, page 13, http://pmodwrc.ch/annual_report/2012_PMODWRC_Annual_Report.pdf, 2012.

Gröbner, J., Kouremeti, N., Nevas, S., Blattner, P., Characterisation Studies of Precision Solar Spectroradiometer, PMOD-WRC Annual Report 2014, p26 http://pmodwrc.ch/annual_report/2014_PMODWRC_Annual_Report.pdf, 2014

Güldner, J.: A model-based approach to adjust microwave observations for operational applications: results of a campaign at Munich Airport in winter 2011/2012, Atmos. Meas. Tech., 6, 2879-2891, doi:10.5194/amt-6-2879-2013, 2013.

Güldner, J. and Spänkuch, D., Remote sensing of the thermodynamic state of the atmospheric boundary layer by ground-based microwave radiometry. Journal of Atmospheric and Oceanic Technology, 18(6), pp.925-933, 2001.

GAW Report-No 231,Fourth WMO Filter Radiometer Comparison (FRC-IV) 28 September-16 October 2015; Davos ,Switzerland, https://library.wmo.int/opac/doc_num.php?explnum_id=3369, WMO, 2016

Halthore, R.N., Eck, T.F., Holben, B.N. and Markham, B.L., , Sun photometric measurements of atmospheric water vapor column abundance in the 940-nm band. Journal of Geophysical Research: Atmospheres, 102(D4), pp.4343-4352, 1997.

Hartmann, D., Klein Tank, A., Rusticucci, M., Alexander, L., Brönnimann, S., Charabi, Y., Dentener, F., Dlugokencky, E., Easterling, D., Kaplan, A., Soden, B., Thorne, P.,Wild, M., and Zhai, P.: Observations: Atmosphere and Surface, in: Climate Change 2013: The Physical Science Basis. Contribution of Working Group I to the Fifth Assessment Report of the Intergovernmental Panel on Climate Change, edited by Stocker, T., Qin, D., Plattner, G., Tignor, M., Allen, S., Boschung, J., Nauels, A., Xia, Y., Bex, V., and Midgley, P., Cambridge University Press, Cambridge, United Kingdom and New York, NY, USA, 2013.

Hong L., Yunchanga C., Xiaominb W., Zhifangb X., Haishena W., Henga H., Meteorological applications of precipitable water vapor measurements retrieved by the national GNSS network of China, Geodesy and Geodynamics, vol 6 no 2, 135-142. http://dx.doi.org/10.1016/j.geog.2015.03.001, 2015.

Holben, B.N., Eck, T.F., Slutsker, I., Tanre, D., Buis, J.P., Setzer, A., Vermote, E., Reagan, J.A., Kaufman, Y.J., Nakajima, T. and Lavenu, F., 1998. AERONET—A federated instrument network and data archive for aerosol characterization. Remote sensing of environment, 66(1), pp.1-16.

Ingold, T., Schmid, B., Matzler, C., Demoulin, P., & Kampfer, N, Modeled and empirical approaches for retrieving columnar water vapor from solar transmittance measurements in the 0.72, 0.82, and 0.94 mu m absorption bands. *Journal of Geophysical Research.*, *105*(D19), 24327–24343. http://doi.org/10.1029/2000JD900392, 2000.

Kasten, F., A new table and approximation formula for the relative optial air mass. Archiv für Meteorologie, Geophysik und Bioklimatologie, Serie B, 14(2), pp.206-223, 1965 .

Kazadzis, S., Kouremeti, N., Diémoz, H., Gröbner, J., Forgan, B. W., Campanelli, M., Estellés, V., Lantz, K., Michalsky, J., Carlund, T., Cuevas, E., Toledano, C., Becker, R., Nyeki, S., Kosmopoulos, P. G., Tatsiankou, V., Vuilleumier, L., Denn, F. M., Ohkawara, N., Ijima, O., Goloub, P., Raptis, P. I., Milner, M., Behrens, K., Barreto, A., Martucci, G., Hall, E., Wendell, J., Fabbri, B. E., and Wehrli, C.: Results from the 4th WMO Filter Radiometer Comparison for

aerosol optical depth measurements, Atmos. Chem. Phys. Discuss., https://doi.org/10.5194/acp-2017-1105, in review, 2017.

Kouremeti, N., Gröbner, J., Spectral Aerosol Optical Depth from a Precision Spectroradiometer, PMOD-WRC Annual Report 2012, p33 http://pmodwrc.ch/annual_report/2012_PMODWRC_Annual_Report.pdf, 2012

Kouremeti, N., Gröbner, J., Spectral Aerosol Optical Depth From a Precision Solar Spectroradiometer During Three Field Campaigns, PMOD-WRC Annual Report 2014, p30 http://pmodwrc.ch/annual_report/2014_PMODWRC_Annual_Report.pdf, 2014

Kouremeti, N., Gröbner, J., Doppler, L., Stability of the Precision Solar Spectroradiometer, PMOD-WRC Annual Report 2015, p40 http://pmodwrc.ch/annual_report/2015_PMODWRC_Annual_Report.pdf, 2015

Marsaglia, G., W. Tsang, and J. Wang. "Evaluating Kolmogorov's Distribution." Journal of Statistical Software. Vol. 8, Issue 18, 2003.

Miloshevich, L.M., Vömel, H., Whiteman, D.N. and Leblanc, T., Accuracy assessment and correction of Vaisala RS92 radiosonde water vapor measurements. Journal of Geophysical Research: Atmospheres, 114(D11), 2009

Nyeki, S., Vuilleumier, L., Morland, J., Bokoye, A., Viatte, P., Mätzler, C., & Kämpfer, N. , A 10-year integrated atmospheric water vapor record using precision filter radiometers at two high-alpine sites. *Geophysical Research Letters*, *32*(23), 1–4, http://doi.org/10.1029/2005GL024079 , 2005.

Pratt, R.W., Review of radiosonde humidity and temperature errors. Journal of Atmospheric and Oceanic Technology, 2(3), pp.404-407, 1985.

Reichard, J., U. Wandinger, M. Serwazi, and C. Weitkamp , Combined Raman lidar for aerosol, ozone and moisture measurements, Opt. Eng., 35, 1457–1465, 1996.

Schneider, M., Romero, P. M., Hase, F., Blumenstock, T., Cuevas, E., & Ramos, R., Continuous quality assessment of atmospheric water vapour measurement techniques: FTIR, Cimel,

MFRSR, GPS, and Vaisala RS92. *Atmospheric Measurement Techniques*, *3*(2), 323–338. http://doi.org/10.5194/amt-3-323-2010,2010.

Schmid, B., Michalsky, J.J., Slater, D.W., Barnard, J.C., Halthore, R.N., Liljegren, J.C., Holben, B.N., Eck, T.F., Livingston, J.M., Russell, P.B. and Ingold, T., Comparison of columnar water-vapor measurements from solar transmittance methods. Applied Optics, 40(12), pp.1886-1896, 2001.

Smirnov, A., Holben, B.N., Eck, T.F., Dubovik, O. and Slutsker, I.,Cloud-screening and quality control algorithms for the AERONET database. Remote Sensing of Environment, 73(3), pp.337-349, 2000.

Smirnov, A, Holben, B.N., Lyapustin A., Slutsker, I. and Eck, T.F., AERONET processing algorithms refinement, AERONET Workshop, El Arenosillo, Spain , May 10 - 14, 2004.

Soden, B.J. and Held, I.M., An assessment of climate feedbacks in coupled ocean–atmosphere models. Journal of Climate, 19(14), pp.3, 2006.

Soden, B. J., and J. R. Lanzante, An assessment of satelliteand radiosonde climatologies of upper-tropospheric water vapor, J. Climate, 9, 1235–1250, 1996.

Swinehart, D.F., The beer-lambert law. J. Chem. Educ, 39(7), p.333 , 1962.

Teillet, P.M., Rayleigh optical depth comparisons from various sources. Applied Optics, 29(13), pp.1897-1900.354-3360, 1990.

Tomasi, C., Vitake, V. and De Santis, L.V., Relative optical mass functions for air, water vapour, ozone and nitrogen dioxide in atmospheric models presenting different latitudinal and seasonal conditions. Meteorology and Atmospheric Physics, 65(1), pp.11-30, 1998.

Vömel, H., Selkirk, H., Miloshevich, L., Valverde-Canossa, J., Valdés, J., Kyrö, E., Kivi, R., Stolz, W., Peng, G. and Diaz, J.A., Radiation dry bias of the Vaisala RS92 humidity sensor. Journal of Atmospheric and Oceanic Technology, 24(6), pp.953-963,2007.

Ware, R., Carpenter, R., Güldner, J., Liljegren, J., Nehrkorn, T., Sol- heim, F., andVandenberghe, F.:Amulti-channel radiometric pro- filer of temperature, humidity and cloud liquid, Radio Sci., 38, 8079, doi:10.1029/2002RS002856, 2003.

Wang, J., Zhang, L., Dai, A., Van Hove, T., and Van Baelen, J.: A near-global, 2-hourly dataset of atmospheric precipitable water from ground-based GPS measurements, J. Geophys. Res., 1 12, D11107, doi:10.1029/2006JD007529, 2007.

Westwater, E. R., Crewell, S., Mätzler, C., and Cimini, D.: Principles of surface-based microwave and millimeter wave radio- metric remote sensing of the troposphere, Quaderni della Societa Italiana di Elettromagnetismo, 1, 50–90, 2005.

WMO/GAW: Experts workshop on Global Surface-based Networkm for long term observations of column aerosol optical properties,Davos, Switzerland, 8–10 March 2004. GAW report No. 162,WMO TD No. 1287, 153 pp., available at: http://www.wmo.int/pages/prog/arep/gaw/gaw-reports.html (last access: 21 October 2016), 2005,

WMO/GAW Report No. 231, The Fourth WMO Filter Radiometer Comparison (FRC-IV), November 2016

Yu, S., Alapaty, K., Mathur, R., Pleim, J., Zhang, Y., Nolte, C., Eder, B., Foley, K. and Nagashima, T., Attribution of the United States “warming hole”: Aerosol indirect effect and precipitable water vapor. Scientific reports, 4, 2014.

Table 1. Statistics of differences among retrievals from PSR using Monochromatic Approach at 946 nm, and retrievals from other instruments for the whole dataset.

	N	*MEAN (CM)*	*STANDARD DEVIATION(CM)*	*MEDIAN (CM)*	*PERCENTILE 10-90 (CM)*	*MEAN RELATIVE (%)*	*R^2*
CIMEL	3501	-0.16	0.18	-0.14	-0.30 -0.04	-3.3	0.92
GPS	2507	0.01	0.17	0.01	-0.11 0.14	0.4	0.94
MWP	2964	-0.05	0.17	-0.04	-0.16 0.07	-0.4	0.95
RS	414	-0.41	1.03	-0.10	-1.42 0.22	-2.7	0.79

Formatted Table

Formatted: English (US)

Table 2. *Statistics of differences among retrievals from PSR using Spectral Approach at 934-948 nm window, and retrievals from other instruments for the whole dataset.*

	N	*MEAN (CM)*	*STANDARD DEVIATION (CM)*	*MEDIAN (CM)*	*PERCENTILE 10-90 (CM)*	*MEAN RELATIVE (%)*	R^2
CIMEL	3501	-0.11	0.07	-0.10	-0.23 -0.02	-0.7	0.97
GPS	2507	0.05	0.10	0.04	-0.06 0.18	0.4	0.97
MWP	2964	-0.04	0.10	0.01	-0.12 0.12	0.3	0.98
RS	414	0.04	0.18	0.02	-0.13 0.25	0.5	0.95

Lexicon

AERONET	AErosol RObotic NETwork
AOD	Aerosol Optical Depth
CIMEL	Sunphotometer Cimel CE318 used in AERONET network
DWD	Deutscher Wetterdienst (German Meteorological Service)
GPS	Global Positioning System
IWV	Integrated Water Vapor (water vapor column)
MODTRAN RTM	MODerate resolution atmospheric TRANsmisson Radiative Transfer Model
MOL-RAO	Meteorologisches Observatorium Lindenberg – Richard Assmann Observatorium
MWP	Microwave Radiometer Profiler
PMOD/WRC	Physikalisch-Meteorologisches Observatorium Davos / World Radiation Center
PFR	Precision Filter Radiometer
PSR	Precision Solar spectroRadiometer
RH	Relative Humidity
RS	Meteorological Radiosondes
WMO	World Meteorological Organisation

Page 21: [1] Deleted **Panagiotis Raptis** **17/01/2018 18:48:00**